Volume 18, Number 4, 2025. pp. 551-560

Jordan Journal of Physics

ARTICLE

Results of Observations for Three Confirmed Exoplanets Using UV/IR Cut Filter

Mohammad F. Talafha[a], **Abdelrazek M. K. Shaltout**[b], **Ali G. A. Abdelkawy**[b] and **. M. Beheary**[b]

[a] *Sharjah Academy of Astronomy, Space Sciences and Technology SAASST, University of Sharjah, UAE.*

[b] *Department of Astronomy and Meteorology, Faculty of Science, Al-Azhar University, Cairo, Egypt.*

Doi: **https://doi.org/10.47011/18.4.11**

Received on: 08/10/2024; *Accepted on: 10/12/2024*

Abstract: We present the exoplanet transit phenomena detected by the Sharjah Astronomical Observatory (SAO-M47) located in Sharjah, United Arab Emirates. In this work, we observed the transits of three hot Jupiter exoplanets, TrES-1b, WASP-104b, and HAT-P-54b, using a UV-IR cut filter with a bandwidth range from 420 to 685 nm. The obtained results were compared with data from a previously published paper and other observations conducted with several filters to identify differences in the analysis of these three hot Jupiter exoplanets. In general, the study focused on how changes in a planet's size are influenced by the particles in its atmosphere. Obtained by using a wide-band UV-IR cut filter and multiwavelength observations, this work's results are comparable to the previous work, specifically regarding the relationship between fine and large particles and the detected scattering effect by blocking the host star light. Several other parameters, such as orbit inclination (i) and transit duration T_{dir}, are also presented with the obtained results, namely, 1.205 ± 0.019 R_{JUP}, 1.028 +0.046 / -0.049 R_{JUP}, and 1.079+0.040/-0.042R_{JUP} for TrES1b, HAT-P-54b, and WASP-104b, respectively. The rest of the parameters are included in the tables.

Keywords: Exoplanet, HAT-P-54b, WASP-104b, TrES-1b, Sharjah Astronomical Observatory (SAO), Photometry transit.

Introduction

Transit photometry is considered the most functional method for detecting distant planets that transit between a star and the Earth. Conducted with this method, regular observations of giant exoplanets are necessary to improve their parameters and ephemerides, thereby assisting in explaining their peculiarities. When a planet crosses (or transits) in front of its parent star's disk, the observed brightness of the star is noticed to drop by a small amount. The depth of transit depends on the relative sizes of the star and the planet [1]. This method of detection is called transit photometry. The transit method enables us to measure the radius of a planet, its inclination, impact parameter, and transit time. The transit of exoplanets allows us to test planetary structure and evolution theories [2].

Observational astronomy becomes science only when we can start to answer questions quantitatively: How far away is that object? How much energy does it emit? How hot is it? The most fundamental information we can measure about celestial objects past our solar system is the amount of energy, in the form of electromagnetic radiation, that we receive from that object. This quantity we will call the flux. The science of measuring the flux we receive from celestial objects is called photometry [3].

Corresponding Author: Mohammad F. Talafha **Email**: mtalafha@sharjah.ac.ae

In the search for extrasolar planets, many methods such as direct imaging, radial velocity, and gravitational lensing have been employed, but the transit method, also known as transit photometry, has proven to be mankind's most effective tool, as it has been responsible for the discovery of exoplanets. Of the 4108 confirmed planets as of the end of January 2020, 3160 were detected using this technique (NASA Exoplanet Archive) (https://exoplanetarchive.ipac.caltech.edu).

In 1992, the first exoplanets around the pulsar PSR B1257+12 were discovered by the detection of the anomalies in the pulsation period [4]. Since then, many amateur astronomers have attempted to measure the signature light-curve dips of known transiting exoplanets in the early 21st century, such as HD209458b [1] and TrES-1b [1, 5], and have reached more than 5700 exoplanets by the year 2024.

There are many techniques used in transit photometry observations to extract more information about the planets, such as defocusing and multiwavelength observations. Here, we used a wide-band filter covering the near-ultraviolet to far-red range (420 – 685 nm) to examine the light curve shape compared with the previous results obtained by using narrow-band or specific filters. The light dispersion depends on the particle size under Mia and Rayleigh scattering methods. From this relationship, we can infer which particle sizes are dominant in the atmosphere.

Target Selection and Observation

We present here the selection and observation of three target exoplanets, chosen according to several specific criteria. The first criterion was to select exoplanets with a transit depth greater than 0.01 mag, as listed in the Exoplanet Transit Database (ETD) (http://var2.astro.cz/ETD). Currently, the Exoplanet Transit Database [6], run by the Czech Astronomical Society since 2009, is the largest repository of such data, containing over 10,000 transit light curves for more than 350 exoplanetary systems [6, 7]. The second condition required that each observation cover the entire transit event, beginning at least 30 minutes before and after the predicted transit interval. The third one was that the target exoplanet be positioned at a high altitude in the sky, corresponding to minimal airmass. Finally, the fourth condition required that the host star's magnitude not exceed 14 mag, which defines the detection limit for the SAO. Based on these conditions, three targets were selected: TrES-1b, WASP-104b, and HAT-P-54b. **TrES-1b** is an exoplanet discovered by the Trans-Atlantic Exoplanet Survey [5]. It is located approximately 512 light-years from the Sun and orbits its host star at a semi-major axis of 0.0393 ± 0.0011 AU [8]. The initially published transit depth was 0.0208 mag [6], and the host star has an apparent V magnitude of 11.79 and is classified as a K0V-type star. TrES-1b lies in the constellation Lyra [5] and has a radius of 1.08 R_{JUP}, a mass of 0.729 M_{JUP}, an orbital period of 3.03 days, and an orbital inclination of 88.2 degrees [9].

HAT-P-54b was discovered and confirmed in 2015 and is among the lowest-mass stars known to host a Hot Jupiter exoplanet, located at a distance of 443 ± 11 light-years [10, 11]. Its transit depth is 0.0265 mag [6], and it orbits a K-dwarf star with an apparent magnitude of V = 13.5. The planet has a radius of 0.944 ± 0.028 R_{JUP}, a mass of 0.760 ± 0.032 M_{JUP}, an orbital period of 3.7998 days, and an orbital inclination that reaches up to 88.04 degrees.

Finally, **WASP-104b** located at a distance of 466 ± 33 light-years, consists of a single star–planet system. Its transit depth is 0.0158 mag [6], and the host star has a V magnitude of 11.1, classified as a G8 main-sequence star [12]. WASP-104b has a radius of 1.1 R_{JUP} [12], a mass of 1.3 M_{JUP}, and an orbital inclination of 83.63 degrees [6]. It is a hot Jupiter that orbits its host star in a circular path with a period of 1.75 days. All the information is displayed in Table 1.

TABLE 1. Reference parameters of the target exoplanets and their host stars.

Targets	TrES-1b	HAT-P-54b	WSAP-104b
R_{JUP}	1.08	0.944±0.028	1.1
M_{JUP}	0.729	0.760±0.032	1.3
Inclination(degree)	88.2	87.04	83.63
Orbital period (Day	3.03	3.7998	1.76
Depth of transit (mag)	0.0208	0.0265	0.0158
Host star (mag)	11.79	13.505	11.1
Host star (Distance Ly)	512	433±11	466±33
Classification of host star	K0V	K	G8

Increasing capabilities of instruments and skills allow amateur astronomers to engage in the exoplanet discovery race and follow-up observations using the transit method, along with university and professional astronomers, in searching for new transiting exoplanets. As an increasing number of submeter-aperture telescopes become employed in these searches, it is important to quantify the detection levels that can be attained with such equipment and to identify analytically methods that can be used to detect and characterize transit light curves [5]. Sharjah Astronomical Observatory (SAO-M47) [25] contains a 0.431m robotic telescope, which makes the observatory unique in the Middle East region, where there are no other professional observatories equipped with similar specialized instruments. Moreover, the robotic telescope is fully automated and protected by a four-meter-diameter dome equipped with a weather station. The telescope is a PlaneWave CDK17 Schmidt-Cassegrain reflector attached to a 4k x 4k SBIG 16803 CCD camera with a filter wheel containing JOHNSON/BESSEL U, B, V, R, and I filters. SAO was built in SAASST for educational purposes, serving undergraduate students throughout the UAE. The University of Sharjah has opened opportunities for students pursuing an M.Sc. degree in Astronomy and Space Sciences, and it plays a vital role in supporting graduate students who are enrolled in this program to conduct their research.

Table 2 presents the log of photometric observations, including the target name, dates of observation, exposure time, number of frames, and photometric precision (SNR). The same observational procedures and analysis methods were applied to all three targets (TrES-1b, HAT-P-54b, and WASP-104b), except for the exposure time. For the analysis described here, only complete transit light curves were used, acquired under conditions determined by the observatory location and the high altitude of the targets in the sky, approximately 50 degrees above the horizon.

Observation planning was based on the Exoplanet Transit Database (ETD) [6], which provided the exact time and date of each transit, as well as the azimuth, altitude of the targets, and other necessary information for following the transit. A UV–IR cut filter (4200–6850 Å) was used for all observations.

Data acquisition and analysis were carried out in two steps. First, MaximDL software was used for telescope guiding, image capture, and reduction. In the second step, the data were analyzed to generate light curves and exoplanet parameters using ManuWin and AstroImageJ software.

TABLE 2. Log of target observations.

Parameters	TrES-1b	HAT-P-54b	WASP-104b
Date of observation	16th June 2018	8th Dec.2018	6th Feb. 2019
Number of Frames	73	29	59
Exposure Time	120sec	300sec	120sec
Filter	UV-IR cut	UV-IR cut	UV-IR cut
Binning	1x1	1x1	1x1
Airmass (min – max)	1.06 – 1.18	1.03 – 1.2	1.05 – 1.15
SNR	~1000	~500	~1000

Observing TrES-1b:

Within the American Association of Variable Star Observers (AAVSO) and transit search networks, many astronomers - expert and amateur - report exoplanet transit light curves and share their results with one another [5]. These data are also published in the Transit Exoplanet Database (TED), as was done for our observations.

TrES-1b was discovered by the Trans-Atlantic Exoplanet Survey (TrES) and is located at coordinates R.A. 19h 04m 09.8s, Dec. +36° 37′ 57″ (J2000) [13].

Our observations of TrES-1b began on 16 June 2018 at 20:20:28 UT (JD 2458286.3475462962) and continued until the last image at 23:26:43 UT (JD 2458286.4910300928). The mid-transit time (TC) occurred at 21:55:22 UT (HJD 2458286.41612 ± 0.00057). An exposure time of 120 s was used to increase the signal-to-noise ratio. Observations started 25 minutes before ingress and ended 15 minutes after egress. A total of 73 images were obtained during the observation period, as shown in Fig. 1.

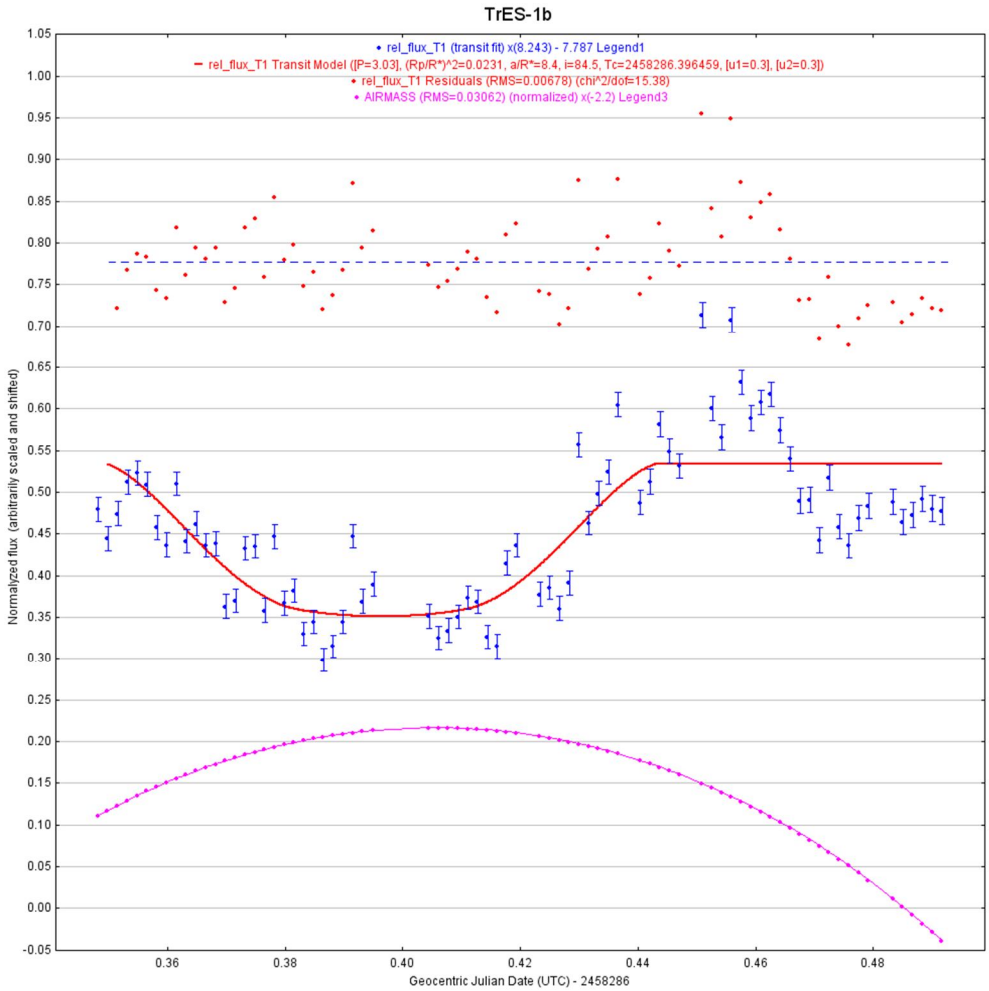

FIG. 1. Top: Residuals of the fitted data. Middle: The best solution for the transit of TrES-1b. Bottom: Air mass during the observation.

Observing HAT-P-54b:

Following the breakdown of two of its orientation wheels, the Kepler space telescope was repurposed in a mission called K2 [10]. In this mission, the Kepler space telescope was utilized to observe 10 fields along the ecliptic plane over a span of two years. For various reasons, the number of stars that can be seen in each field is significantly lower than in the first Kepler mission. Due to this, early perceptions of K2 fields by ground-based telescopes to pre-select targets are very beneficial [10]. The exoplanet HAT-P-54b is in the primary field that can be seen by the K2 mission, known as Feld 0. This planet, found by the HATNet study, is the first transiting planet identified in this field [10]. Initial photometric observations of the star HAT-P-54 were carried out by the fully automated HATNet system [10]. It was found that the radius of HAT-P-54b is smaller than 92% of the known transiting planets with masses greater than that of Saturn [11]. The host star has V = 13.505 ± 0.060, a mass of 0.645 ± 0.020 M_{sun} and a radius of 0.617±0.01 R_{sun}, making HAT-P-54 one of the lowest-mass stars known to host a hot Jupiter [10]. HAT-P-54 was observed by Sharjah Observatory on 8 December 2018. The first image was taken at 20:31:16 UT (JD 2458486.3475462962), with the ingress of the transit occurring at 21:06:00 UT at an altitude of 82° (E), giving an ingress duration of 35 minutes. The last image was taken at 23:22:06 UT (2458486.4910300928 JD), resulting in an egress duration of 25 minutes at an altitude of 75° (W). The mid-transit time was observed at 22:12:44 UT (Tc = 2458461.42204 ± 0.00134 HJD) [6], as shown in Fig. 2.

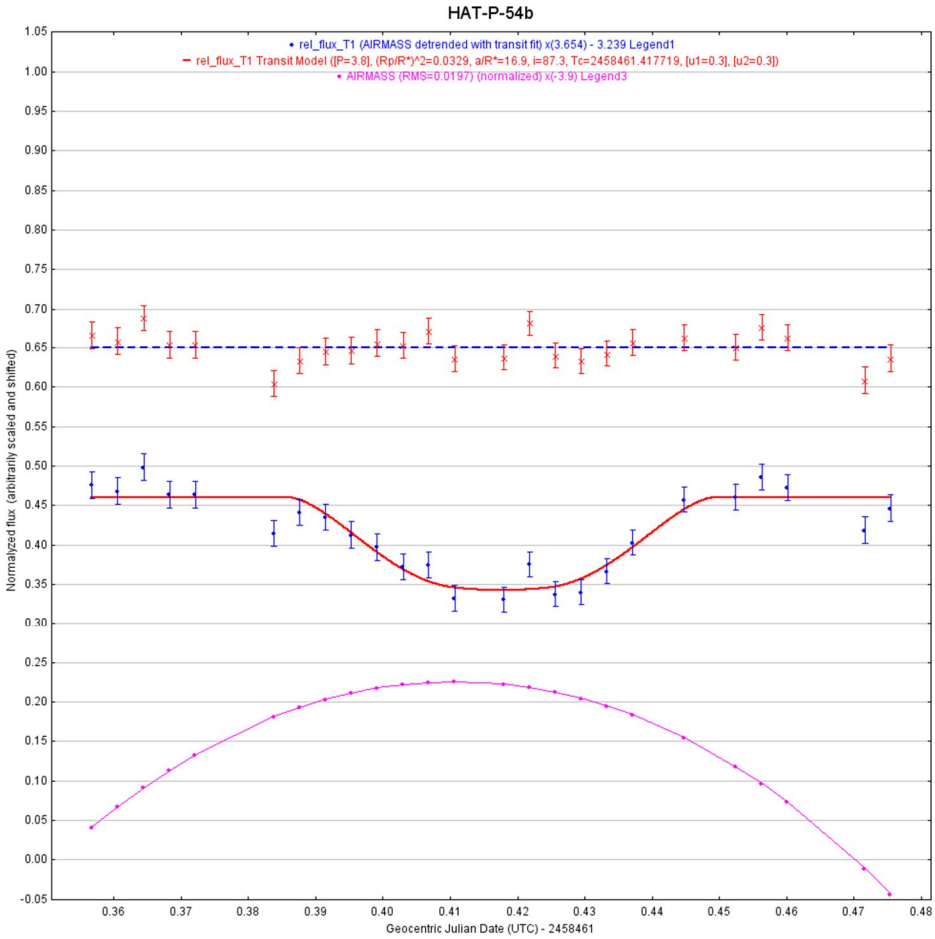

FIG. 2. Top: Residuals of the fitted data. Middle: The best solution for the transit of HAT-P-54b. Bottom: Air mass during the observation.

Observing WASP-104b:

Information regarding planets transiting stars that are brighter than those observed by Kepler is required to expand our knowledge of the range of properties exhibited by the nearby planets, as well as to advance our understanding of planetary formation and evolution [14]. WASP-104b is a transiting hot Jupiter in a 1.76-day circular orbit around a V = 11.1 G8 main-sequence star. The planet has a mass of 1.3 M_{JUP} and a radius of 1.1 R_{JUP} [12].

Sharjah Astronomical Observatory was successful in observing the full transit of WASP-104b on 6 February 2019. Observations started at 19:31:13 (2458521.3133449075JD) with the first touch of the transit beginning at 20:21 (63 SE), meaning that it took 50 minutes for ingress. The last image was at 22:37:01 (2458521.4423726853 JD). The egress of the transit was at 22:06 UT (72 S), making it ~30 minutes after egress of the transit. The mid of the transit was at 21:14 (Tc = 2458521.37323 ± 0.00101JHD) [6] at an altitude of 71 S. A long exposure time (120 sec) was used for raising the SNR, with the best value of SNR achieved in image 14 (SNR ~1010 and 1/SNR ~ 0.001). The light curve appears with 59 images during the observation period, as shown in Fig. 3.

Analysis and software:

For analyzing and creating the light curve, two different software packages were used. First, the Muniwin package was employed to produce the light curve based on the observed magnitude dip. The optimal aperture photometry was selected for processing, with careful choice of comparison stars. The results were saved as a .txt file and submitted to the TRESCA transit model on the Exoplanet Transit Database (ETD) website [6] (http://var2.astro.cz/ETD/observers.php) to calculate exoplanet parameters and plot the light curves. The air mass curve and the fitted transit observations in the TRESCA model were used to derive the parameters for our observational light curves, which are presented in Table 3.

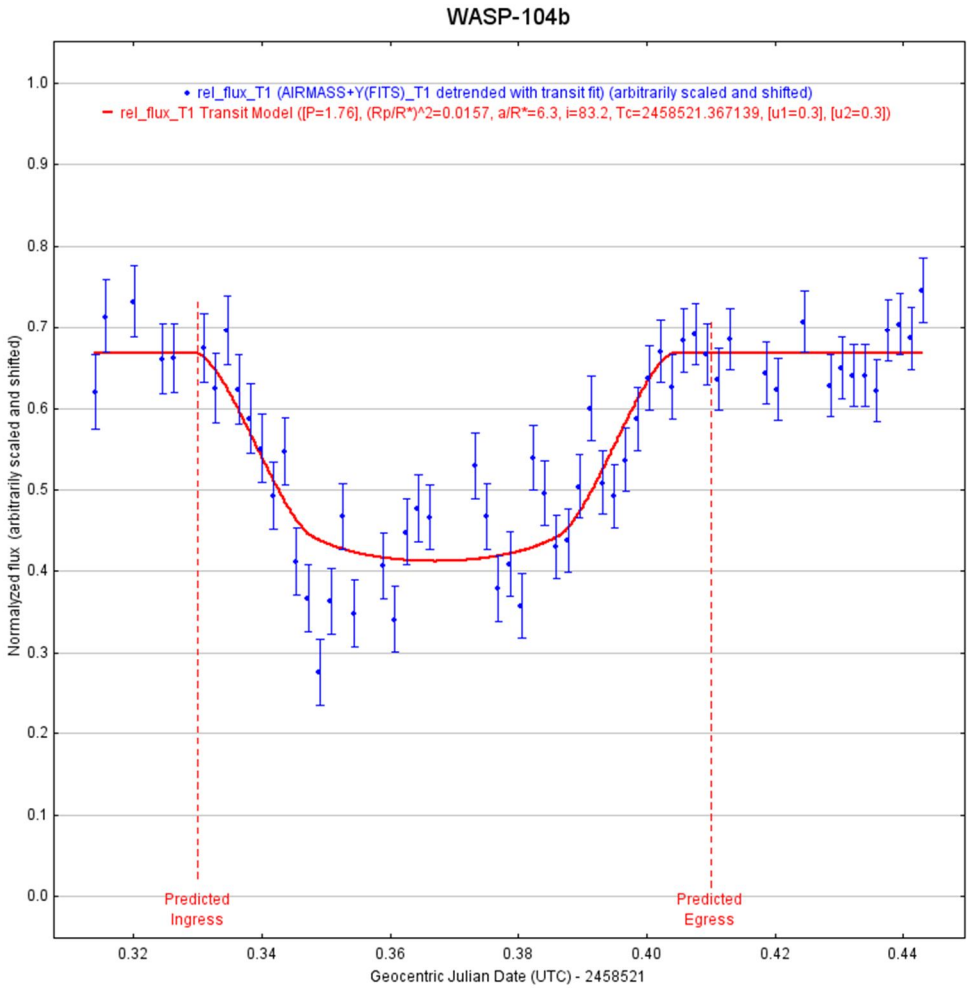

FIG. 3. Top: Residuals of the fitted data. Middle: The best solution for the transit WASP-104b. Bottom: Air mass during the observation.

TABLE 3. Parameters and observational solutions generated by the Exoplanet Transit Database (TRESCA) model.

Targets & Parameters	TrES-1b	HAT-P-54b	WASP-104b
Orbit inclination(i)	87.65◦	86.53◦	88.67°
Transit depth (mag)	0.0249± 0.0008	0.0321± 0.003	0.0144± 0.0011
Transit duration (min)	144.8± 2	95.9± 6	99.2± 4
R of planet (R_{JUP})	1.205	1.028	1.079
Fit data	2	3	3

The second software used for calculations was AstroImageJ, which allows fitting and plotting of the data [15]. In this software, some parameters, such as the host star radius and the planet period, are fixed. Figure 1 shows the light curve of the exoplanet's full transit, with the fitted data overlaid, alongside the air mass curve to illustrate the observing conditions. The red in the legend lists the transit solution numbers for this transit. The same applies to Figs. 2 and 3.

Discussion:

Observing the primary transit of an exoplanet at multiple wavelengths allows researchers to investigate the composition and structure of its atmosphere. The measured Rp/R∗ depends on the opacity of the planetary atmosphere and thus allows for useful insights into the atmosphere's spectral features and composition. If the opacity in the near-UV band is dominated by Rayleigh scattering of molecular hydrogen, it may be possible to place strong upper limits on the planet's 10-bar radius [16]. The apparent size of the planet is determined from the flux dip

relative to the out-of-transit flux, as shown in Figure 4. The star magnitude varies when different filters are used. In our observations, using a wide wavelength filter, such as a UV-IR cut filter (420 – 865 nm), Fig. 5, the magnitude should decrease or the flux increase. On the other hand, the exoplanet does not play a part in the change in magnitude related to the flux; rather, it will show more wavelength blocking depending on the atmosphere's particle size. Axiomatically, it is independent of the different magnitudes of the host star before and during the transit. The wavelength-dependent transit depth indicates the atmosphere composition of an exoplanet [17]. Differences, such as asymmetric transit shapes, longer durations, or significantly deeper transit depths (>∼1%) compared to the optical filter [16], provide direct evidence of the significant effects of using wide-band filters, particularly in the blue and near-UV wavelengths.

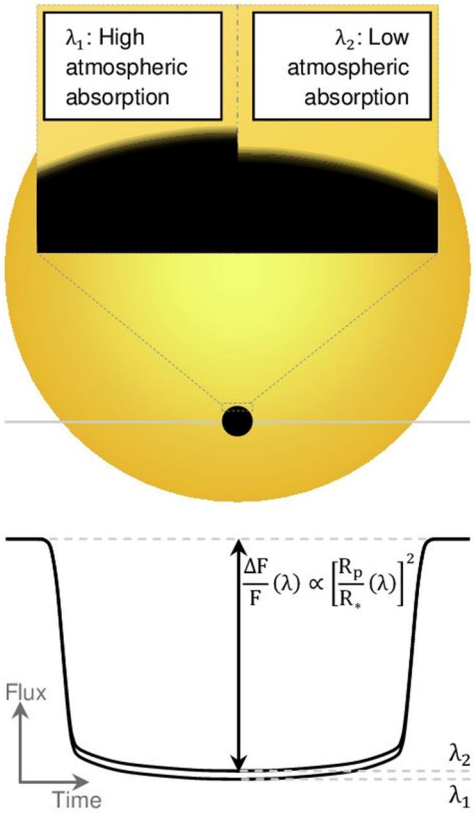

FIG. 4. Transit-depth variations, ΔF/ F (λ), caused by the wavelength-dependent opacity of a transiting planet's atmosphere. The stellar disk and planet are unresolved; the observed flux variation corresponds to a point source [24].

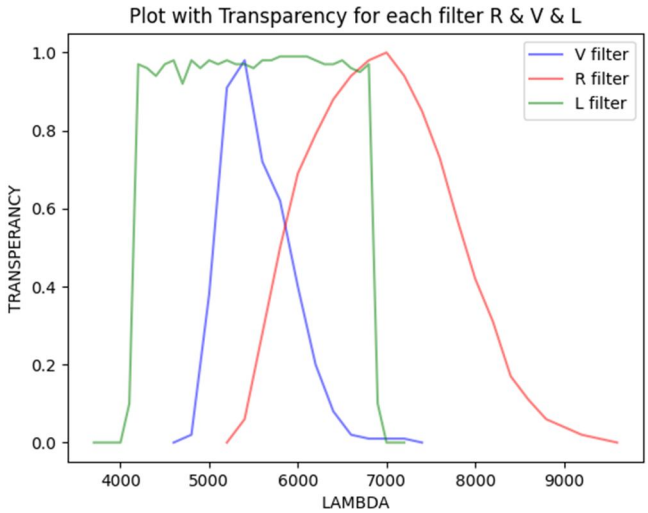

FIG. 5. Filter transparencies: R-Red, V-Visual, and L- Luminous.

This band allows us to determine the correlation between fine and large particles in the exoplanet's atmosphere by comparing the planet's size using the R and L filters. The observed visible size from a single observation is provided in Table 4. Based on this, we can estimate the distribution, amount, and concentration of particles spread around the planet. These particles are necessarily small and light because Rayleigh scattering is more effective than Mie scattering, as shown in Fig. 6. These results demonstrate the significant effects of using a wide-band filter, especially in the blue and near-UV wavelengths. This band allows us to assess the correlation between fine and large particles in the exoplanet's atmosphere by the ratio of the planet's size measured with the R and L filters, with the net visible size from a single observation summarized in Table 4.

TABLE 4. Comparison of (R p / R s) results from multiwavelength observations with those from this work.

HAT-P-54b			TrES-1b			WASP-104b		
Filter	Transit depth	References	Transit depth	Filter	Reference	Transit depth	Filter	Reference
V	0.15616	[19]	0.1382	V	[20]	0.124	V	[21]
I	0.16898	[19]	0.13686	z	[22]	0.129	R	[21]
R	0.17516	[19]	0.08	Ks	[23]	0.12140	I, z	[14]
L	0.18133	This Work	0.15218	L	This Work	0.12512	L	This Work
Expected literature value	0.1572	[10]	0.130	R	[8]	0.121	R	[12]

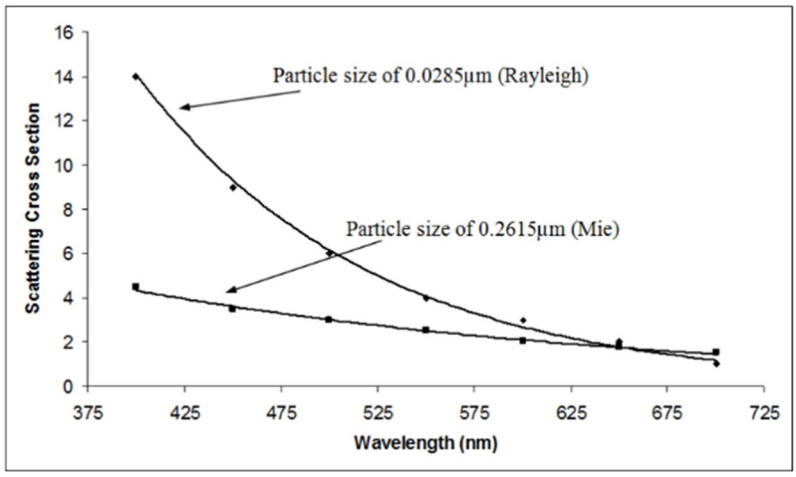

FIG. 6. Effects of Rayleigh and Mie scattering cross sections as a function of wavelength for different particle sizes [26].

These types of observations are indispensable for further investigations of exoplanet atmospheres and for comparisons with planets in the Solar System, such as recent studies combining CHEOPS and TESS data to examine differences in transit depths. The authors summarize several factors that affect transit depth; by default, variations in measured exoplanet size arise from differences in the sensitivity of the TESS and CHEOPS instruments, as well as the effects of limb darkening at shorter wavelengths, to which CHEOPS is more sensitive than TESS [18]. We know that stellar magnitudes vary when observed through different filters. Using a wide-band filter, such as a UV–IR cut filter (420–865 nm), the observed magnitude should be equal to or lower than that obtained with a narrow-band filter, and the measured flux should be the same or higher. The exoplanet itself does not directly affect this change in magnitude; rather, the observed flux variation reflects wavelength-dependent blocking by particles in the planet's atmosphere. This effect is independent of the host star's magnitude before or during the transit. Based on these observations, we can estimate the distribution, quantity, and concentration of particles surrounding the planet. These particles are necessarily small and light, as Rayleigh scattering is more effective than Mie scattering, as shown in Fig. 6. Near-UV transits may also exhibit asymmetries in their light

curves, including differences in ingress/egress timing, asymmetric transit shapes, longer durations, or significantly deeper transit depths (>1%) compared to observations in the optical [16].

TrES-1b:

- The orbit inclination is lower by 0.5°
- The planet radius obtained from the transit solution is large by around 10%.
- The larger radius of the planet leads to the conclusion that it is of a lower density.

HAT-P-54b:

- The orbit inclination is lower by 0.5°
- The planet radius obtained from the transit solution is larger by around 9%.
- The larger radius of the planet leads to the conclusion that it is of a lower density.

WASP-104b:

- The orbit inclination is higher by 0.5°.
- The planet radius obtained from the transit solution is almost similar to the previously published values.

Conclusion

In this paper, we investigated the capability of the Sharjah Optical Observatory in observing and detecting the transit of exoplanets. Despite the light-polluted location, we were able to observe and detect the transit. Our results show a clear match with the results from the previous observations and confirm the Jupiter-type exoplanets. Even under the difficult observation conditions, such as light pollution, low-latitude sites, and non-clear atmosphere, exoplanets can still be observed and confirmed. We demonstrate that exoplanet transits can be observed from suboptimal sites using relatively small telescopes. Our observatory is fully capable of observing exoplanets, even though it is located within a city with a high level of light pollution. Notably, the Sharjah Optical Observatory is the first observatory in the Gulf region to successfully observe exoplanets. Moving forward, we aim to expand our efforts to observe more exoplanets through transit photometry and to incorporate spectroscopy, providing training opportunities for students and establishing a community of exoplanet observers in the region.

Acknowledgements

We would like to extend our sincere gratitude to Spencer Mung, an IAESTE intern at the Sharjah Academy for Astronomy, Space Sciences, and Technology, for his invaluable efforts in editing, and to Ms. Nora Alamiri, Eng.Trifa al-Kaabi, Eng. Ibrahim Al-Sabt, Ms. Asmaa Alhameed, and Mr. Ahmad Al-Hariri for their assistance in review and editing. This research is based on data from the ETD database and makes use of the SIMBAD database via the Astrophysics Data Abstract Service. The authors are also grateful to the anonymous referee for their valuable notes and recommendations.

References

[1] Barkaoui, K. et al., J. Phys.: Conf. Ser., 869 (2017) 012073.

[2] Shporer, A. et al., ApJ, 690 (2009) 1393.

[3] Romanishin, W., "An Introduction to Astronomical Photometry Using CCDs", (Rochester, NY, 2002).

[4] Rabus, M. et al., Astron. Astrophys., 508 (2) (2009) 1011.

[5] Bissinger, R., Soc. Astron. Sci. Ann. Symp., 24 (2005) 81.

[6] Poddaný, S. et al., New Astron., 15 (3) (2010) 297.

[7] Kokori, A., ApJS, 258 (2) (2022) 40.

[8] Alonso, R. et al., ApJ, 613 (2) (2004) L153.

[9] Laughlin, G. et al., ApJ, 621 (2) (2005) 1072.

[10] Bakos, G.A. et al., AJ, 194 (4) (2015) 149.

[11] Kjurkchieva, D.E. et al., Serb. Astron. J., 198 (2019) 55.

[12] Močnik, T. et al., AJ, 156 (2) (2018) 44.

[13] Price, A. et al., J. Am. Assoc. Var. Star Obs., 34 (2005) 1.

[14] Smith, A.M. et al., Astron. Astrophys., 570 (2014) A64.

[15] Collins, K.A. et al., AJ, 153 (77) (2017) 1.

[16] Turner, J.D. et al., Mon. Not. R. Astron. Soc., 459 (1) (2016) 789.

[17] Yang, F. et al., Astrophys. Space Sci., 366 (2021) 83.

[18] Gaidos, E. et al., Mon. Not. R. Astron. Soc., 468 (3) (2017) 3418.

[19] Saha, S. et al., AJ, 162 (1) (2021) 18.

[20] Narita, N. et al., Publ. Astron. Soc. Jpn., 59 (4) (2007) 763.

[21] Valyavin, G.G. et al., Astrophys. Bull., 73 (2018) 225.

[22] Winn, J.N. et al., ApJ, 657 (2007) 1098.

[23] Adams, E.R. et al., AJ, 146 (1) (2013) 9.

[24] De Wit, J. and Seager, S., Science, 342 (6165) (2013) 1473.

[25] Talafha, M.F., Shaltout, A.M., Abdelkawy, A.G., and Beheary, M.M., New Astronomy, 119 (2025) 102379.

[26] Bin Omar, A.F. and Bin MatJafri, M.Z., Sensors, 9 (10) (2009) 8311.